ELSEVIER

Journal of Immunological Methods 231 (1999) 207–222

JOURNAL OF IMMUNOLOGICAL METHODS

www.elsevier.nl/locate/jim

Extended half-life and elevated steady-state level of a single-chain Fv intrabody are critical for specific intracellular retargeting of its antigen, caspase-7

Quan Zhu [a,*], Congmei Zeng [a], Alexandra Huhalov [a,1], Jin Yao [a], Thomas G. Turi [b], Dennis Danley [b], Thomas Hynes [b], Yang Cong [b], Debra DiMattia [b], Scott Kennedy [b], Gaston Daumy [b], Eric Schaeffer [b], Wayne A. Marasco [c,d], James S. Huston [a]

[a] *IntraImmune Therapies Inc., P.O. Box 15599, Boston, MA 02215-0011, USA*
[b] *Pfizer Central Research, Groton, CT 06340, USA*
[c] *Department of Cancer Immunology and AIDS, Dana-Farber Cancer Institute, Boston, MA 02115, USA*
[d] *Department of Medicine, Harvard Medical School, Boston, MA 02115, USA*

Abstract

Two single-chain Fv (sFv) antibodies (C8 and H2) specific for Mch3/caspase-7, a component in the signaling pathway for induction of apoptosis, were genetically fused to different intracellular targeting signals and analyzed by expression in mammalian cells. Immunofluorescence microscopy confirmed that these anti-caspase-7 intrabodies were expressed in the cellular compartments dictated by their C-terminal trafficking signals. Cytosolic caspase-7 was successfully retargeted to different subcellular compartments by specific intrabodies through direct association of antigen with intrabody. Sequestration of caspase-7 in nuclei had a significant biological impact in that the expression of a nuclear-targeted anti-caspase-7 intrabody in a stable Jurkat cell line markedly inhibited staurosporine-induced apoptosis. The criteria for choosing an optimal intrabody were also evaluated in this study. A gene dosage titration study demonstrated that the C8 intrabody was more potent in retargeting of caspase-7 than the H2 intrabody, even though the H2 sFv had a higher affinity for caspase-7 than the C8. Pulse-chase experiments and western blot analysis revealed that the anti-caspase-7 C8 sFv intrabodies exhibited a long half-life (>8 h) and high steady-state levels of protein accumulation, while the H2 intrabodies had a half-life of 2 h and less protein at steady state. These results suggest that the choice of sFv as an intrabody depends critically on the intracellular sFv protein having an extended half-life and elevated steady-state level. Thus, extended half-life must be considered together with sFv antibody specificity and affinity when choosing an optimal sFv intrabody for functional studies of cellular proteins.
© 1999 Elsevier Science B.V. All rights reserved.

Keywords: sFv intrabody; Protein turnover; Intracellular targeting; Caspase-7; Apoptosis

Abbreviations: ER, endoplasmic reticulum; Fv, $V_H + V_L$ domains of an antibody; HA, the influenza hemagglutinin epitope YPYDVPDYA; nls, the SV40 large T-antigen nuclear localization signal; PBS, phosphate buffered saline; PCR, polymerase chain reaction; SEC, size-exclusion chromatography; sFv, single-chain Fv; SV40, simian virus 40; V_H, the variable domain of an antibody heavy chain; V_L, the variable domain of an antibody light chain

* Corresponding author. E-mail: quanzhu@tiac.net

[1] Present address: Department of Oncology, Royal Free Hospital and University College School of Medicine, Rowland Hill Street, London NW3 2PF, UK.

0022-1759/99/$ - see front matter © 1999 Elsevier Science B.V. All rights reserved.
PII: S0022-1759(99)00158-1

1. Introduction

In the last decade molecular immunology has enormously expanded our understanding of how antibodies are made naturally and how to make them artificially through antibody engineering (Haber, 1992; Huston et al., 1996). Advances in a number of laboratories have provided ready access to the Fv region, the minimal antibody binding site, which is formed by non-covalent association of the V_H and V_L variable domains. The Fv has proven most useful as a single gene product in the form of the single-chain Fv (sFv), where the V_H and V_L are joined by a flexible polypeptide linker (Bird et al., 1988; Huston et al., 1988). The recent development of human sFv-phage libraries has allowed high affinity human sFv antibodies to be selected at will from combinatorial libraries that contain billions of different combining sites (Marks et al., 1991; for reviews see Winter et al., 1994; Marks and Marks, 1996).

Antibody engineering has made it possible to manipulate the genes encoding antibodies and to express antibody binding sites, in forms such as the sFv, within mammalian cells. Intracellular antibodies, termed intrabodies, can be genetically fused with known intracellular protein trafficking signals and thereby be directed to different subcellular compartments, resulting in modulation of the target function by degradation, inhibition, or sequestration. Intrabodies have been used successfully for both phenotypic and functional knockouts of target molecules (for recent reviews, see Marasco, 1997; Jones and Marasco, 1998; Pelegrin et al., 1998), suggesting they hold promise for gene therapy and basic research applications, such as target validation and functional genomics.

The first sFv intrabody study demonstrated that expression of an sFv against gp120, the human immunodeficiency virus (HIV) envelope protein, within the endoplasmic reticulum (ER) blocked gp120 processing and its incorporation into virions (Marasco et al., 1993). Blockade of gp120 diminished virus-mediated syncytium formation and reduced the infectivity of progeny HIV particles. Intrabodies targeted to the lumen of the ER were subsequently used to inhibit the expression and the function of the erbB-2 transmembrane tyrosine kinase protein (Beerli et al., 1994; Deshane et al., 1994; Deshane et al., 1995a,b, 1996, 1997; Graus-Porta et al., 1995), which is overexpressed in a variety of human tumors, most notably certain breast and ovarian cancers. ER-targeted sFv intrabodies were also utilized to downregulate cell surface expression of the α chain of the interleukin 2 receptor (IL-2R α) (Richardson et al., 1995, 1997), the CD2 T cell marker (Greenman et al., 1996), the EGF receptor (Jannot et al., 1996), and the VLA-4 integrin (Yuan et al., 1996). Utilizing cytoplasmic sFv intrabodies, several groups were able to abolish functions of cytosolic proteins by either cytoplasmic sequestration of targets such as HIV-1 *tat* (Mhashilkar et al., 1995, 1997) or direct inhibition of the protein activity in the case of c-Ras (Biocca et al., 1993, 1994; Werge et al., 1994; Montano and Jimenez, 1995; Cochet et al., 1998), HIV-1 reverse transcriptase, integrase and matrix protein (reviewed in Rondon and Marasco, 1997).

This study is part of an effort to expand the application of intrabodies in target validation and functional genomics. Toward this end, we investigated the utility of intrabody technology to explore the functional requirements for proteins involved in apoptosis. Caspase-7 is a 34 kd cytosolic protein and a member of the CED3/ICE cysteine protease/caspase family, which comprises important mediators of apoptosis (see recent reviews in Cohen, 1997; Nicholson and Thornberry, 1997). Utilizing anti-caspase-7 sFv intrabodies, this investigation finds that the cytosolic human recombinant caspase-7 could be retargeted to either the nuclei or peroxisomes of transfected cells depending upon which intracellular trafficking signal was attached to the intrabodies. Furthermore, this investigation evaluated factors that govern efficient retargeting of caspase-7 by the intrabodies. Our results also demonstrate that intrabody-mediated transfer of the caspase-7 protein from its normal location in the cytosol to the nucleus caused functional change that yielded impairment of the apoptotic signaling pathway.

2. Materials and methods

2.1. Single-chain Fv selection

A very large phage display library (Cambridge Antibody Technology, Cambridge, England) was

used to derive two genetically distinct human single-chain Fv (sFv) antibodies against caspase-7 (Vaughan et al., 1996). The sFv genes from this library are in the form of a V_H-linker-V_L, where the linker consists of the $(Gly_4Ser)_3$ fifteen residue linker (Huston et al., 1988). C8 sFv was selected using a peptide representing the N-terminal 19 amino acids of caspase-7 p20 subunit as described (Cong et al., manuscript in preparation). The other sFv, H2, was selected using a bacterially produced full length GST-procaspase-7 (C186A) mutant protein. The construction and bacterial expression of GST-procaspase-7 (C186A) are described elsewhere (Cong et al., manuscript in preparation). Purified GST-procaspase-7 (C186A) was coated onto Maxisorp immunotubes (Nunc, Naperville, IL) at a concentration of 50 μg/ml. Three rounds of selection were carried out using published protocols (Vaughan et al., 1996). To reduce the occurrence of GST binding clones, purified GST was included in solution at a concentration of 100 μg/ml during the incubation of the library phage with the immobilized GST-procaspase-7 (C186A). Clones from the second and third round of selection were screened for binding to the antigen by ELISA. The unique positive clones were identified by restriction enzyme mapping, confirmed by DNA sequencing, and subcloned into pUC-119 for expression and purification. No further epitope mapping data was available for H2 sFv. The control sFv antibody, C3, was also selected from the same phage display library against a mammalian cytosolic protein that is an irrelevant target for the present study.

2.2. Bacterial expression of sFv and in vitro sFv-antigen affinity measurements

Both sFv were over expressed in *Escherichia coli* and purified as described (Cong et al., manuscript in preparation). The purified proteins were characterized by SDS-PAGE, western blot analysis, N-terminal amino acid sequencing, size exclusion chromatography (SEC), and matrix assisted laser desorption ionization mass spectroscopy (MALDI-MS).

Kinetic constants for the binding interaction between H2 sFv and GST-procaspase-7 (C186A) antigen were determined by surface plasmon resonance on a BIAcore (BIAcore, Piscataway, NJ) as described for C8 sFv (Cong et al., manuscript in preparation). Briefly, anti-His antibody (Qiagen, Valencia, CA) was chemically immobilized onto CM5 biosensor chips (BIAcore, Piscataway, NJ). The sFv, harboring the His tag, was captured onto the antibody surface followed by injections of various concentrations of the GST-procaspase-7 (C186A) antigen. The data from the sensorgrams were analyzed and globally fitted using BIAevaluation 3.0 software (BIAcore, Piscataway, NJ).

2.3. Plasmid construction

pcDNA3.1(+) (Invitrogen, Carlsbad, CA) was modified by inserting a PCR fragment containing 5′*Nhe*I–*Asc*I–*Sfi*I–*Nco*I-stufferDNA–*Not*I-HA tag-Stop codon-*Pac*I–*Xba*I 3′ between *Nhe*I and *Xba*I sites of the vector to generate pcDNA-stuffer-HA. The stuffer DNA, about 400 bp in length, serves the purpose of a space filler. The sequence of the stuffer DNA will be available upon request. The nucleotide sequence of the forward primer used in this PCR was: 5′CTA GCT AGC TAG GCG CGC CAA GGC CCA GCC GGC CAT GGA GCT CAA GAT GAC ACA GAC TAC ATC C3′. The nucleotide sequence of the reverse primer used was: 5′CCT CTA GAT TAA TTA ATT ACG CGT AGT CTG GGA CGT CGT ATG GGT ATG CGG CCG CTA CAG TTG GTG CAG CAT C3′. With identical forward primer 5′caa gct ggc tag cta ggc g 3′, the following three constrcucts were created: the SV40 large T-antigen nuclear targeting sequence PKKKRKV (Kalderon et al., 1984) was introduced into pcDNA-stuffer-HA by PCR using the reverse primer: 5′-TCC GAT CTT TAA TTA ACT AAA CCT TAC GTT TCT TCT TCG GCG GAG TCG CGT AGT CTG GGA CGT C-3′, generating pcDNA-stuffer-HA-nls, where nls stands for the SV40 nuclear localization signal; the major peroxisomal targeting signal peptide SKL (Gould et al., 1989; Keller et al., 1991; Wiemer et al., 1997) was introduced into pcDNA-stuffer-HA by PCR using the reverse primer: 5′-TCC GAT CTT TAA TTA ACT ACA GTT TAC TCG CGT AGT CTG GGA CGT C-3′, generating pcDNA-stuffer-HA-SKL; and the endoplasmic reticulum retention signal peptide SEKDEL (Munro and Pelham, 1987) was introduced into pcDNA-stuffer-HA by PCR using the reverse primer: 5′-TCC GAT CTT TAA TTA ACT ACA GCT CGT CCT TTT CGC TCG CGT

AGT CTG GGA CGT C-3′, generating pcDNA-stuffer-HA-KDEL. pcDNA-stuffer-Cκ-HA was created by insertion of the entire human kappa chain constant domain (Cκ) into the *Not*I/*Pac*I sites of pcDNA-stuffer-HA. The stuffer DNA in pcDNA-stuffer-HA vector, pcDNA-stuffer-HA-nls vector, the pcDNA-stuffer-HA-SKL vector, pcDNA-stuffer-HA-KDEL, and pcDNA-stuffer-Cκ-HA vector was replaced with the *Sfi*I/*Not*I DNA fragment encoding either C8 or H2 anti-caspase-7 sFv genes from phage display vector pUC119, which generated the sFv intrabody constructs of C8 sFv-HA, C8 sFv-nls, C8 sFv-SKL, C8 sFv-KDEL, C8 sFv-Cκ-HA, H2 sFv-HA, H2 sFv-nls, H2 sFv-SKL, H2 sFv-KDEL, and H2 sFv-Cκ-HA. Note that all of the C8 and H2 sFv constructs contained the influenza hemagglutinin epitope YPYDVPDYA, representing the HA tag and expression of the intrabodies are under the control of the cytomegalovirus (CMV) promoter (Fig. 1).

Caspase-7 with a C-terminal fusion of the FLAG epitope tag (DYKDDDDK, Hopp et al., 1988) was constructed by ligation of a *Bam*HI/*Eco*RI digested DNA fragment encoding caspase-7 with a similarly digested pcDNA3.1 vector containing a FLAG epitope. The DNA fragment containing caspase-7 was generated by PCR using the forward primer: 5′ GGA TCC ACG ATG GCA GAT GAT CAG GGC 3′ and the reverse primer: 5′ GAA TTC AAC TGA CTT CAT CTC AAG GAA CC 3′ with pcDNA3-caspase-7 as a template. The expression of caspase-7-FLAG is driven by the same CMV promoter as the intrabodies.

2.4. Cell lines

The hamster kidney cell line, BHK-21, and human embryonic kidney transformed epithelial cell line, 293T, were cultured in Dulbeco minimal essential medium (DMEM, Gibco/BRL, Gaithersberg, MD) supplemented with 2 mM L-glutamine and 10% fetal calf serum at 37°C, 5% CO_2. The human T-cell leukemia cell line, Jurkat, was grown in RPMI 1640 medium (Gibco/BRL) supplemented with 25 mM HEPES, 2 mM glutamine, 1 × non-essential amino acids, and 10% fetal calf serum at 37°C, 5% CO_2.

2.5. Transient transfection

Transient transfection of BHK-21 cells were carried out with the LipofectaminePlus reagent from Gibco BRL according to the manufacturer's instructions. For immunofluorescence experiments, 5×10^4 cells were seeded onto one cover slip per well in 6-well plates. 2 μg DNA including the sFv intrabody and the caspase-7 plasmids were transfected into cells on the next day with 3 μl of Lipofectamine and 10 μl of the Plus reagent. For western blot measurements of steady-state levels of sFv intrabody expression and for the coimmunoprecipitation experiments, $0.5–1.0 \times 10^6$ cells were seeded onto 100 mm plates.

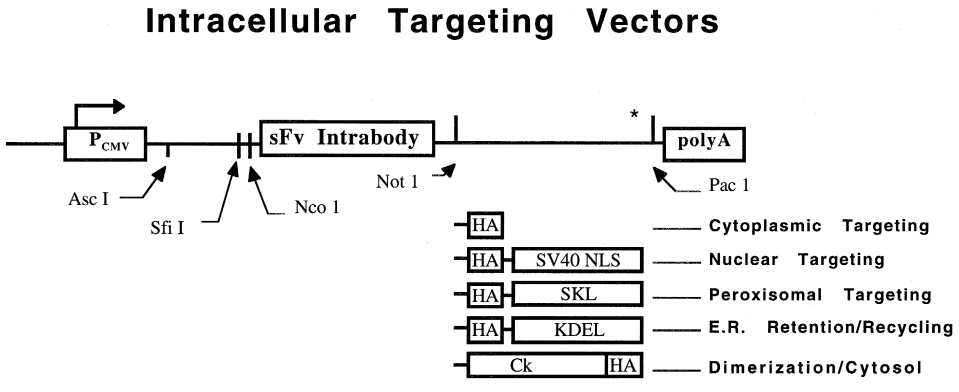

Fig. 1. Intrabody targeting vectors. The vectors were designed to accept sFv genes from standard sFv-phage libraries, in which sFv genes are flanked by Sfi I and Not I restriction sites. A set of vectors was prepared in which the region flanking the Not I site made the expressed sFv into a fusion protein that contained the hemagglutinin tag (HA), followed by sequences encoding a trafficking signal C-terminal to the HA tag. The expression of the sFv intrabody is mediated by the CMV promoter.

15 μg DNA (sFv and caspase-7) were transfected into cells with 40 μl of Lipofectamine and 40 μl of Plus reagent the next day. Cells were incubated with the DNA/LipofectaminePlus mixture for 3 h at 37°C. The mixture was then removed and replaced with fresh growth medium. Cells were grown at 37°C, 5% CO_2 until assay time.

Transient transfection of 293T cells were performed with Superfect reagent from Qiagen (Valencia, CA) according to manufacturer's instructions. For pulse-chase experiments, 3×10^5 cells were seeded per well in 6-well plates. The mixture of DNA and Superfect reagent contained 3 μg DNA (2 μg sFv plasmids) diluted in 150 μl serum-free DMEM medium with 15 μl Superfect, which was mixed with 900 μl of complete medium before addition to cells. Cells were incubated with the DNA/Superfect mixture for 3 h at 37°C. Upon removal of the mixture, cells were washed once with PBS and incubated with fresh growth medium at 37°C, 5% CO_2 until assay time.

For all transfections, pMTGH, a control plasmid that encodes human growth hormone (hGH),was co-transfected with the sFv intrabody constructs and/or the caspase-7 construct for normalization of the transfection efficiency. The expression level of the transfected hGH was determined from growth media at the time for cell assays using the hGH ELISA Kit from Boehringer Mannheim (Indianapolis, IN) according to the manufacturer's instructions.

2.6. Immunofluorescence microscopy

At about 44 h post-transfection, BHK-21 cells were washed with PBS and fixed with 4% paraformadehyde at room temperature (RT) for 30–45 min. Upon fixation, cells were permeabilized with 0.2% Triton X-100 for 5 min at RT and blocked with PBS containing 10% normal goat serum and 5% BSA for 30 min. Anti-HA polyclonal antibody, Y-11, from Santa Cruz Biotechnology (Santa Cruz, CA) was used as the primary antibody for detecting sFv intrabodies at a concentration of 0.1 μg/ml. Anti-FLAG M2 monoclonal antibody purchased from BAbCO (Richmond, CA) was used as the primary antibody to detect caspase-7-FLAG fusion protein at a concentration of 2.8 μg/ml. A sheep anti-human catalase polyclonal antibody (The Binding Site, San Diego, CA) was used to visualize cellular peroxisomes. Cells were incubated with the primary antibodies for 1 h at RT. FITC-conjugated goat anti-rabbit IgG (Sigma, St. Louis, MO)was used at 1:400 dilution as the secondary antibody to stain for sFv intrabodies and rhodamine-conjugated goat anti-mouse IgG (Pierce, Rockford, IL) was used at 1:400 dilution to stain for caspase-7-FLAG. The incubation of cells with the secondary antibodies was for 1 h at RT. DAPI (4′,6-diamidino-2-phenylindole, Sigma), a fluorescent probe for DNA binding, was used to stain nuclei when necessary. Cells were incubated with 0.5 μg/ml of DAPI in PBS for 5 min at room temperature. After washing with PBS, the coverslips were mounted in Vectashield H-1000 mounting medium (Vector Laboratories, Burlingame, CA) on glass slides. The immunostained cells were examined with an Olympus AX70 fluorescence microscope and photographed using its auto-exposure mode. The pictures were processed and printed using Adobe Photoshop.

2.7. Co-immunoprecipitation and western blot analysis

About 44 h post transfection, nearly confluent transiently transfected BHK-21 cells were lysed on 100 mm culture plates in 1 ml 50 mM Tris (pH 8.0) containing 100 mM NaCl, and 0.25% IGEPAL CA-630 (Sigma) for 60 min on ice. Upon centrifugation in a microcentrifuge for 10 min at 14,000 rpm, 1 ml supernatants were incubated with 40 μl of the anti-FLAG M2 monoclonal antibody affinity resin (BAbCO, 50% slurry). After being gently washed twice in the same buffer, the immunoprecipitated proteins were separated by SDS-PAGE on a 12% gel and transferred to a nitrocellulose membrane. Western blot analysis was performed sequentially, first with 0.2 μg/ml anti-HA polyclonal Y-11 antibody and then with 5.6 μg/ml anti-FLAG M2 antibody. HRP-conjugated secondary antibody (Sigma) and ECL kits from Amersham (Arlington Heights, IL) were used to visualize sFv and caspase-7 specific protein bands. When steady-state levels of the sFv intrabody were studied, the cellular supernatant was treated directly with SDS-PAGE sample buffer and proteins were separated by SDS-PAGE followed by western blot analysis.

2.8. Intrabody protein turnover analysis

For the pulse-chase experiments, $1–2 \times 10^6$ cells of transiently transfected 293T cells were incubated with 1 ml of methionine/cysteine-free medium for 2 h at 37°C and then metabolically labeled with the same medium containing 400 μCi/ml [^{35}S]methionine/cysteine (DuPont NEN, Boston, MA) for 30 min at 37°C. Immediately after labeling, the cells were washed 2 times with 1 ml DMEM medium supplemented with 10% FCS, 2 mM L-glutamine, 40× excess methionine (1.2 mg/ml) and 20× cysteine (0.84 mg/ml) (chase medium) and incubated with the same medium for various times. At each time point, cells were washed twice with cold PBS and lysed with 200 μl lysis buffer (1% Triton X-100, 0.5% deoxycholate, 0.1% SDS, 150 mM NaCl, 50 mM Tris, pH 8.0) containing proteinase inhibitors (50 μg/ml Aprotinin, 50 μg/ml Leupeptin, and 1 mM PMSF) on ice for 10 min. After removing cell debris by centrifugation, the supernatants were immunoprecipitated with the anti-HA monoclonal antibody, HA.11, (1:200 dilution, BAbCO) in the lysis buffer with 400 mM NaCl at 4°C overnight. Upon 2 h incubation with protein G resin (Gibco BRL) at 4°C, the resin with bound antibody/protein complexes was washed 5 times with the lysis buffer containing 400 mM NaCl. The immunoprecipitated proteins were then treated with SDS-PAGE sample loading buffer and separated by SDS-PAGE (12% polyacrylamide). The gels were dried before autoradiography and quantitation with a PhosphorImager (Molecular Dynamics, Sunnyvale, CA).

2.9. Construction of stably transfected Jurkat cell lines

Jurkat cells (5×10^6) were transfected with 5 μg of either pcDNA3.1 vector, C8 sFv-nls plasmid, C8 sFv-SKL plasmid, or a control intrabody C3 sFv-nls plasmid using Superfect from Qiagen. Two days following transfection, cells were placed in the medium containing 1 mg/ml G418. After about two weeks under G418 selection, no significant cell survival was observed in the control cells transfected without DNA. The cells transfected with the different DNA constructs were diluted and seeded at a density of 100 to 600 cells/well in 96-well plates. Following incubation with G418 for another 10–14 days, cells were picked from the wells containing visibly growing cell clusters. These cells were expanded and tested for intrabody expression using immunofluorescence as well as western blot analysis. The bulk transformants with positive IF staining for intrabodies were subcloned. The cell seeding densities for subcloning were: 10, 1, 0.1 cells/well in 96-well plates. Upon selection and expansion, subcloned cell lines were tested again for intrabody expression by immunofluorescence. The positive cell lines were analyzed further by pulse-chase experiments to evaluate the stability of the intrabody.

2.10. Cell survival assay

Approximately 2×10^6 cells from each individual stably transfected Jurkat cell line were treated with 2 μM staurosporine (Sigma) in serum-free RPMI 1640 media for 18 h at 37°C, 5% CO_2. The survival of each cell line following 18 h treatment was determined by Trypan Blue staining. The percentage of cells excluding Trypan Blue, indicating survival, was recorded in the presence or absence of staurosporine.

3. Results

3.1. Expression and characterization of the sFv intrabodies

Two genetically distinct anti-caspase-7 single-chain Fv (sFv) genes, C8 and H2, were isolated from a phage antibody library as discussed in Section 2. The bacterially expressed, purified C8 sFv preparation appeared homogeneous by a variety of biochemical criteria (Cong et al., manuscript in preparation). The purified H2 sFv preparation also appeared homogeneous, affording a single monomeric species by SEC and SDS-PAGE (data not shown) with expected N-terminal sequence and total mass as determined by MALDI-MS (expected 28048 dalton, observed 28033 dalton). Characterization of association between bacterially produced C8 sFv or H2 sFv and caspase-7 showed that the H2 sFv preparations exhibited a higher affinity for the GST-procaspase-7 (C186 A) antigen than the C8 sFv preparation (Table 1). Both

Table 1
Characteristics of the anti-caspase-7 sFv*

Anti-caspase-7 sFv	C8**	H2
K_D (nM)	224.6 ± 18	14.2 ± 2.5
$k_{on} \times 10^3$ (M^{-1} s^{-1})	13.8 ± 0.2	98.5 ± 2.9
$k_{off} \times 10^{-3}$ (s^{-1})	3.1 ± 0.2	1.4 ± 0.3
Half-life	> 8 h	2 h
Effect on re-directing caspase-7	+ + + +	+

* The error shown for tabulated values represent propagated error in the calculation, based on 95% confidence limits on measured values.
** Kinetic values from Cong et al., Isolation and characterization of a blocking single chain antibody for the processing of procaspase-7. Manuscript in preparation.

anti-caspase-7 sFv genes were cloned into *Sfi*I and *Not*I sites of the intrabody vectors shown schematically in Fig. 1.

Cellular expression of the anti-caspase-7 sFv intrabodies was first analyzed by immunofluorescence microscopy of transiently transfected BHK-21 cells. About 44 h post-transfection, the cells were fixed, permeabilized, and stained with the anti-HA antibody. As shown in Fig. 2, the anti-caspase-7 C8 sFv-nls and H2 sFv-nls were localized in the nuclei. Cells transfected with C8 sFv-SKL (Fig. 2 i–l) and H2 sFv-SKL (data not shown) had punctate staining patterns similar to that seen with the cellular catalase, which is mainly localized in peroxisomes. C8 sFv-HA and H2 sFv-HA intrabody proteins, devoid of any specific targeting signal, were detected in the cytosol (Fig. 2 a, b, e, and f). These data indicate that the anti-caspase-7 sFv intrabodies were expressed in the expected subcellular compartments as dictated by their C-terminal intracellular trafficking

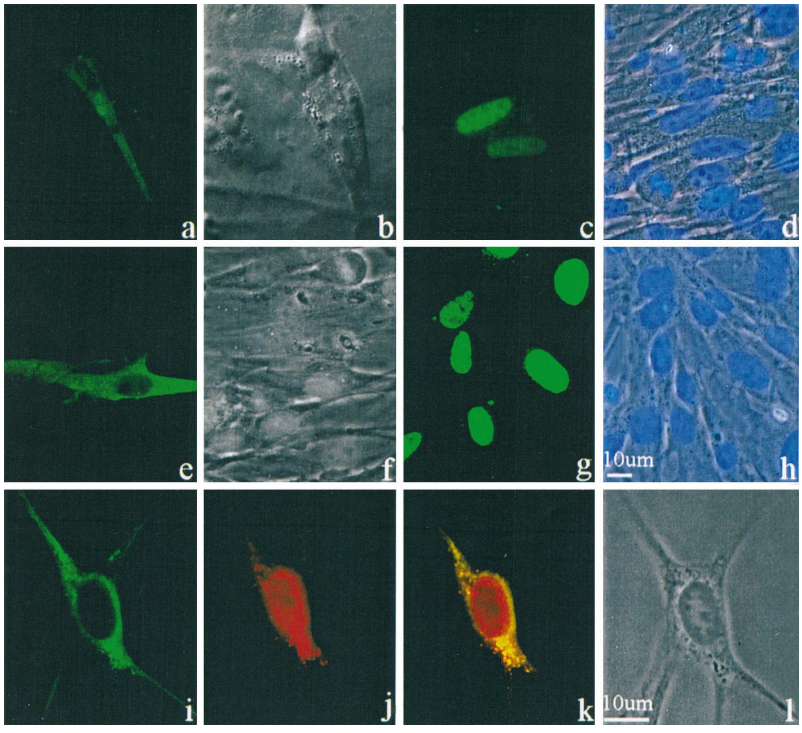

Fig. 2. Immunofluorescence microscopy of the anti-caspase-7 sFv intrabody transiently transfected BHK-21 cells. BHK-21 cells transfected with plasmids encoding H2 sFv-HA (a and b), H2 sFv-nls (c and d), C8 sFv-HA (e and f), C8 sFv-nls (g and h), or C8 sFv-SKL (i–l) were fixed and permeabilized. To visualize the subcellular localization of the anti-caspase-7 intrabodies under a fluorescent microscope, cells were reacted with the anti-HA monoclonal antibody, HA.11, followed by incubation with an FITC-conjugated goat anti-mouse IgG antibody (a, c, e, g, and i, FITC; b, d, f, h, and l, phase contract). DAPI was used to stain the nuclei of the transfected cells (d and h, phase contract plus fluorescence). To verify the cellular peroxisomes, C8 sFv-SKL transfected cells were also incubated with a sheep anti-human catalase polyclonal antibody and Texas red-conjugated donkey anti-sheep IgG (j). Panel k is the dual image of the same microscope field as in i and j, where a Texas red/FITC dual filter was used.

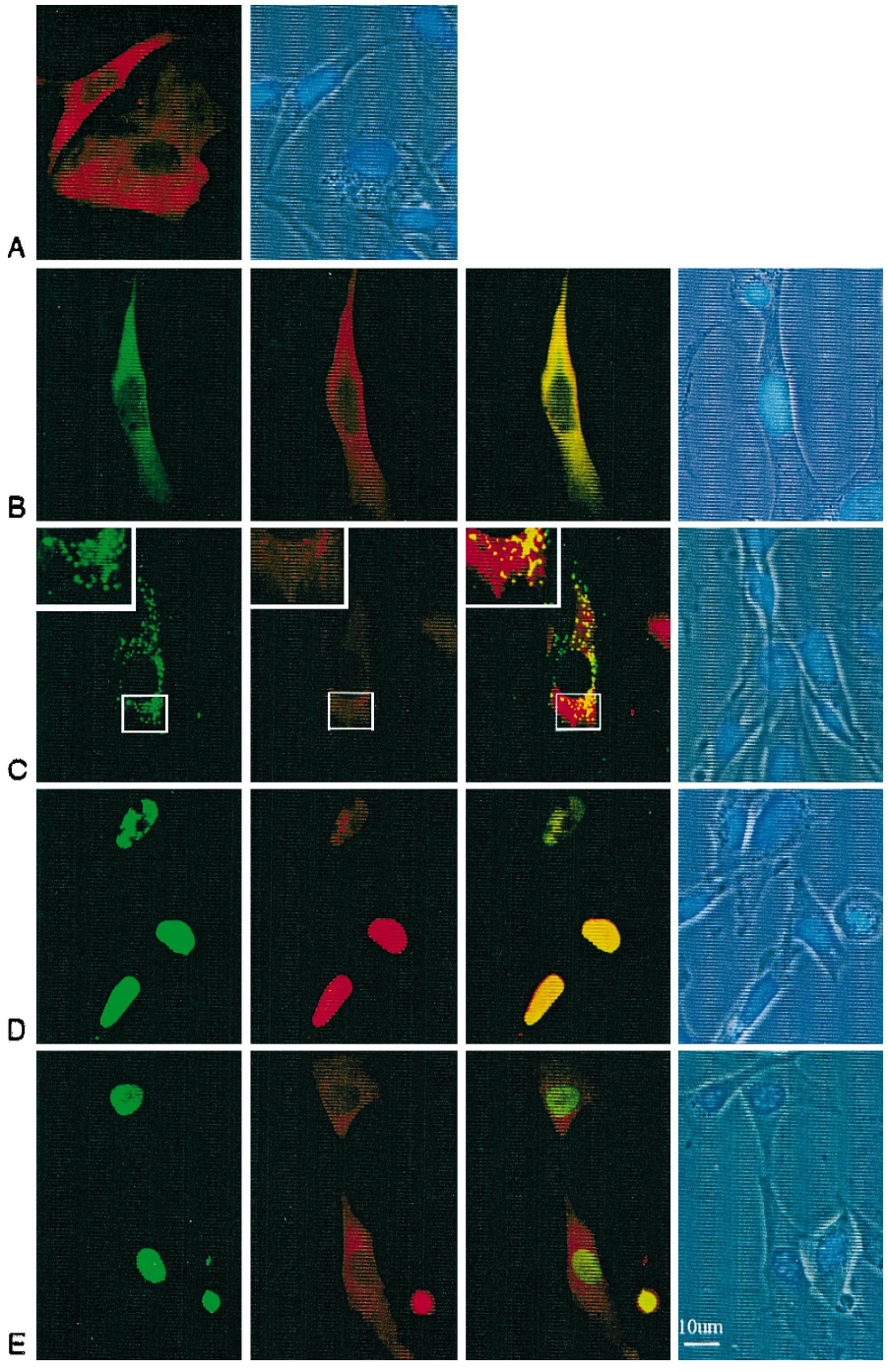

Fig. 3. Dual immunofluorescence analysis of subcellular localization of caspase-7-FLAG in the presence of anti-caspase-7 intrabodies. Caspase-7-FLAG was cotransfected with C8 sFv-HA (Row B), C8 sFv-SKL (Row C), C8 sFv-nls (Row D), or a control intrabody C3 sFv-nls (Row E). In rows B–E, the four columns represent, from the left, FITC-stained intrabody, rhodamine stained caspase-7-FLAG antigen, dual immunofluorescence, and phase contrast/fluorescent (DAPI) image of the same field. Row A shows cytoplasmic localized caspase-7-FLAG in the absence of any cotransfected intrabodies, with rhodamine-stained caspase-7-FLAG at the left and phase contrast/DAPI of the same image at right.

signals. It should be noted that H2 sFv intrabodies in general exhibited weaker fluorescence intensity than their C8 counterpart regardless of their cellular location, suggesting a lower accumulation level of these proteins at steady-state.

3.2. Intracellular retargeting of cotransfected caspase-7 proteins by the sFv intrabodies

The effect of the intrabodies on cotransfected caspase-7 was evaluated in terms of their ability to retarget caspase-7 to different subcellular compartments. Recombinant human caspase-7 protein fused with a C-terminal FLAG-peptide tag was coexpressed with different anti-caspase-7 C8 sFv intrabodies in BHK-21 cells. At 40–44 h post-transfection, the cells were fixed, permeabilized, and stained with the anti-FLAG M2 mouse monoclonal antibody and the anti-HA Y-11 rabbit polyclonal antibody. Using immunofluorescence microscopy, the subcellular localization of the recombinant caspase-7-FLAG protein and its corresponding intrabodies were visualized. Fig. 3 shows that caspase-7-FLAG was a cytoplasmic protein in BHK-21 cells when transfected alone (Fig. 3A) or cotransfected with a cytoplasmic localized C8 sFv-HA intrabody (Fig. 3B). In contrast, peroxisomal punctate staining (Fig. 3C) and nuclear staining (Fig. 3D) of caspase-7-FLAG were observed when caspase-7-FLAG was coexpressed with C8 sFv-SKL and C8 sFv-nls intrabody, respectively. The retargeting of caspase-7-FLAG is due to specific interactions between caspase-7 and anti-caspase-7 sFv intrabodies. This was evident when expression of an irrelevant nuclear targeting sFv intrabody, C3 sFv-nls, failed to retarget cytosolic caspase-7-FLAG to the nucleus (Fig. 3E), demonstrating that a specific antigen-antibody interaction is required for retargeting. The H2 sFv intrabodies could also retarget caspase-7-FLAG to different subcellular compartments, although with much lower efficiency, as discussed later in this section. The immunofluorescent images of retargeted caspase-7-FLAG by H2 sFv intrabodies were similar to those illustrated in Fig. 3 for C8 sFv intrabodies (data not shown).

Interactions between caspase-7 and its specific sFv intrabodies were further investigated by a co-immunoprecipitation assay in conjunction with western blot analysis. BHK-21 cells were transiently transfected with caspase-7-FLAG and either its specific intrabodies, C8 or H2 sFv-nls, or an irrelevant intrabody, C3 sFv-nls. At 44 h post-transfection, cell lysates were prepared and immunoprecipitated with

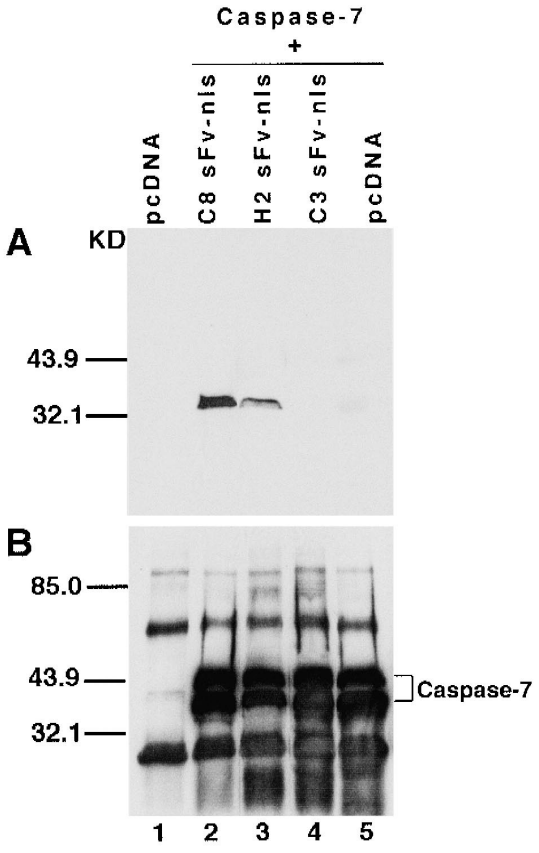

Fig. 4. Co-immunoprecipitation of the anti-caspase-7 sFv intrabodies with caspase-7-FLAG. BHK-21 cells were either transfected with pcDNA (Lane 1) or caspase-7-FLAG alone (Lane 5), or cotransfected with caspase-7-FLAG and C8 sFv-nls (Lane 2), H2 sFv-nls (Lane 3), or a control intrabody C3 sFv-nls (Lane 4). Around 44 h post-transfection, cells were lysed and precipitated with the anti-FLAG M2 antibody. The precipitated proteins were separated by SDS-PAGE and blotted with a polyclonal anti-HA antibody to visualize the intrabodies (panel A). After stripping off the anti-HA antibody, the same blot was incubated with the anti-FLAG M2 antibody to reveal the caspase-7-FLAG protein (panel B). The doublet band of caspase-7-FLAG is an intrinsic property of the caspase-7-FLAG constructs because the same doublet was observed as the product of an in vitro transcription coupled translation reaction (data not shown). The additional protein bands in panel B could be a result of the HRP-conjugated anti-mouse secondary antibody detecting heavy and light chains of the anti-FLAG monoclonal antibody used in immunoprecipitation.

the anti-FLAG M2 monoclonal antibody affinity resin. Proteins bound to the anti-FLAG immunoabsorbant were separated by SDS-PAGE, transferred to a nitrocellulose membrane and analyzed by western blotting with the anti-HA Y-11 polyclonal antibody followed by the anti-FLAG M2 monoclonal antibody. The results in Fig. 4 demonstrate a direct interaction between caspase-7 and its specific intrabodies: with comparable amounts of caspase-7-FLAG precipitated directly using the anti-FLAG antibody (Fig. 4B), anti-caspase-7 C8 and H2 sFv-nls intrabodies could be coprecipitated with the caspase-7-FLAG while no association of the irrelevant C3 sFv-nls intrabodies with caspase-7-FLAG was observed (Fig. 4A).

3.3. Efficiency of intrabody-mediated nuclear retargeting of caspase-7

The overall efficiency of anti-caspase-7 sFv intrabodies on retargeting cytoplasmic caspase-7 to other cellular compartments was assessed quantitatively by plasmid titration assays. Using intrabodies targeted to nuclei as an example, increasing amounts of either C8 sFv-nls or H2 sFv-nls plasmid were cotransfected with a constant amount of caspase-7-FLAG plasmid. The transfected cells were stained with both the anti-HA antibody and the anti-FLAG antibody as described above. Using immunofluorescence microscopy, positively transfected cells were scored for caspase-7-FLAG subcellular distribution categorized as exclusively nuclear, nuclear plus cytoplasmic, and exclusively cytoplasmic. The experiments were performed in duplicate and repeated two times. The average subcellular distribution of caspase-7-FLAG from these experiments was plotted in Fig. 5 as a percentage of each type of cellular localization vs. DNA ratio. The experimental results showed that in a gene-dosage dependent manner, C8 sFv-nls intrabody could efficiently increase the total nuclear staining of caspase-7-FLAG to over 80% with virtually none left in the cytosol. On the other hand, the retargeting of caspase-7-FLAG to nuclei by H2 sFv-nls intrabody was not as efficient. Only about 19% of caspase-7-FLAG staining was exclusively nuclear at an intrabody to caspase-7-FLAG plasmid ratio of 3:1.

3.4. Steady-state expression and turnover measurements of the sFv intrabodies

It was unexpected that the H2 sFv-nls intrabody was less efficient in retargeting caspase-7-FLAG

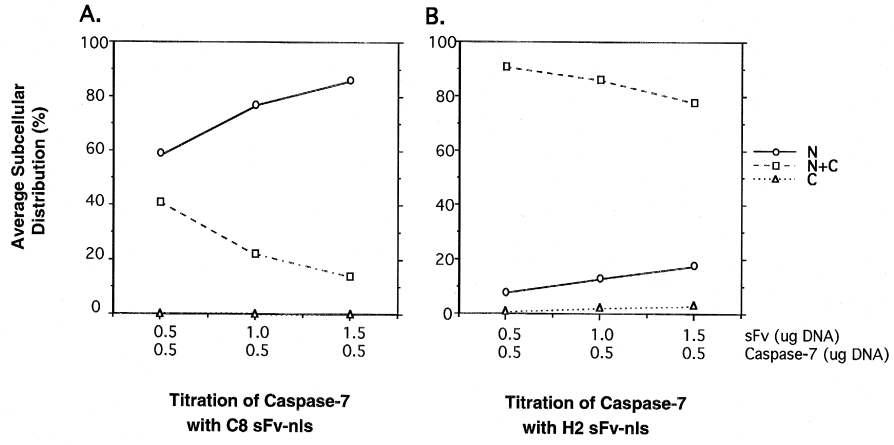

Fig. 5. Gene dosage analysis on the efficiency of caspase-7-FLAG retargeting by C8 sFv-nls and H2 sFv-nls intrabodies. A constant amount (0.5 μg) of caspase-7-FLAG plasmid was cotransfected with increasing amounts of either C8 sFv-nls (panel A) or H2 sFv-nls (panel B) plasmid. Using immunofluorescence microscopy, the subcellular localization of caspase-7-FLAG in the cotransfected cells was scored as exclusively nuclear (N), nuclear and cytoplasmic (N + C), and exclusively cytoplasmic (C). Special efforts were made to ensure that the judgment criteria were identical for C8 sFv-nls and H2 sFv-nls. The data presented are averaged from two experiments performed in duplicate. Over 100 transfected cells stained positive for the caspase-7 were counted for each sample, resulting in a total of 300 to 800 cells counted for the averaged results shown in this figure. The percentage of caspase-7-FLAG subcellular localization in each category is plotted as a function of the increasing dosage of each transfected anti-caspase-7 intrabody plasmid.

antigen as compared to C8 sFv-nls, especially when one considers that H2 sFv intrabodies had a higher affinity (Table 1). To examine whether expression levels influenced the effectiveness of these intrabodies, steady-state levels of the anti-caspase-7 sFv intrabody expression were then analyzed by western blot analysis of transfected BHK-21 cell lysates, with samples taken at 44 h post-transfection. All anti-caspase-7 sFv intrabodies migrated at their expected molecular weights (Fig. 6A). Upon normalization with transfection efficiency (hGH assays as discussed in Section 2, data not shown) and amount of total protein (judged by actin detection, Fig. 6A and protein concentration assay, data not shown), the overall steady-state levels of the H2 sFv intrabody proteins were much less than those of the C8 sFv intrabodies. This result is consistent with our observations using immunofluorescence microscopy, where H2 sFv intrabodies always exhibited weaker fluorescence intensity than their C8 counterpart regardless of their cellular location, again suggesting a lower local concentration H2 sFv intrabodies within cells.

One of the possible explanations of lower steady-state accumulation of the H2 intrabodies could be attributed to protein stability. An sFv intrabody with a very long half-life would persist and potentially reach a much higher steady-state level than one with a very short half-life. To directly examine this hypothesis, turnover rates of the intracellular anti-caspase-7 sFv intrabodies were measured by pulse-chase experiments coupled with immunoprecipitation. At 40 h post-transfection, cells were washed and starved for 2 h. Cellular proteins were then pulse-labeled with ^{35}S-methionine/cysteine and chased with medium containing excess amounts of cold methionine/cysteine. The anti-caspase-7 sFv intrabodies were detected by immunoprecipitation with the anti-HA antibody, HA.11, and separated by SDS-PAGE (Fig. 6B). The average half-lives of the anti-caspase-7 sFv intrabodies were quantitated and the results are summarized in Table 1. Fig. 6B and Table 1 show that all C8 sFv intrabodies were very stable, with a $t_{1/2}$ greater than 8 h. In contrast, all H2 sFv intrabodies had a relatively short half life of about 2 h. Further experiments indicated that the half-lives of the C8 sFv intrabodies were as long as 2–3 days (data not shown). The significant difference in stability of the two anti-caspase-7 antibodies correlates with the protein accumulation at steady-state (Fig. 6A).

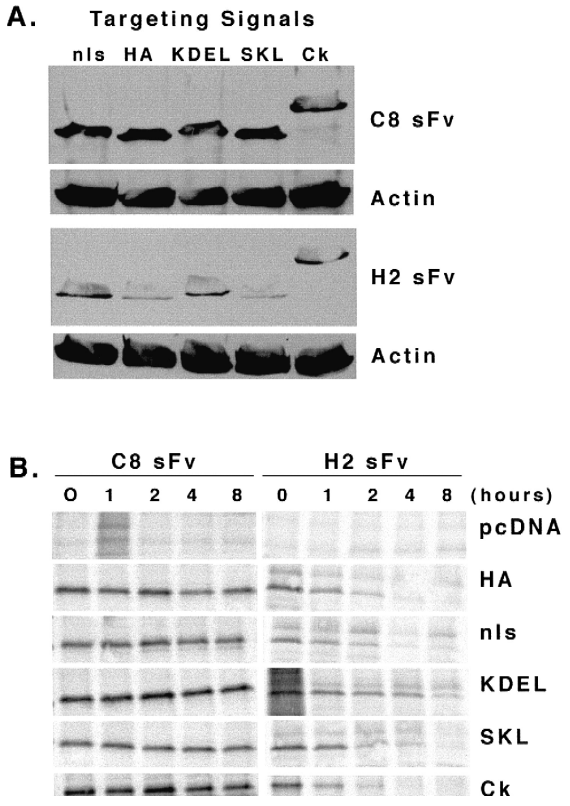

Fig. 6. Expression of the anti-caspase-7 sFv intrabodies in transiently transfected BHK-21 and 293T cells. A. Relative levels of intrabody accumulation in transfected cells assessed by western blot analysis. The C8 (A. upper) and H2 (A. lower) sFv intrabodies with different targeting signals (as labeled on top of each lane) were expressed in transiently transfected BHK-21 cells. Following cell lysis and SDS–polyacrylamide gel electrophoresis, the sFv in extracts was visualized by Western blotting with anti-HA antiserum. The identical blot was also incubated with an anti-actin antibody (Sigma) to visualize cellular actin, which was used as a control antigen. B. Pulse-chase analysis of the anti-caspase-7 sFv intrabody turnover rates in transiently transfected 293T cells. Upon transfection and metabolic pulse-labeling with [^{35}S]-methionine/cysteine for 30 min, cells were lysed following different time of chase and precipitated with the anti-HA antibody. The precipitated proteins were separated by 12% SDS-PAGE and visualized by autoradiography. Chase time in hours are labeled on top and the targeting signal fused to each intrabody is labeled at the right of the gel image.

It should be noted that the half-life and steady-state accumulation seemed to be an intrinsic property of

the sFv protein, which was relatively insensitive to the fused target peptide signal and the subcellular compartment to which it was targeted: cytosol, nucleus, or peroxisomes. To test this hypothesis further, two additional intrabody constructs were made, wherein the sFv was fused with an endoplasmic reticulum (ER) retention signal KDEL (Munro and Pelham, 1987) or a human kappa chain constant domain (Cκ) as a dimerization domain (Mhashilkar et al., 1995). Both the C8 and H2 sFv-KDEL intrabodies were localized within ER as visualized by immunofluorescence (data not shown), demonstrating the effectiveness of the KDEL-receptor-mediated retrieval mechanism (Pelham, 1989). While different intracellular targeting had a negligible effect on the half-life of C8 sFv, the steady-state level of H2 sFv was enhanced when it was targeted to the ER. As shown in Fig. 6, H2 sFv could be readily detected at the 4 h time point when targeted to the ER. Conversely, none of the other subcellular compartments increased the half-life of H2 sFv beyond 2 h. The increased level of H2 sFv within the ER may reflect the higher concentration of chaperon-like proteins found within this compartment (Hammond and Helenius, 1995). Association of these proteins with H2 sFv may stabilize the sFv and extend its half-life. Nonetheless, H2 sFv-KDEL still had much shorter half-life and less steady-state accumulation than that of C8 sFv-KDEL (Fig. 6). Insertion of the human Cκ domain at the C-terminus of the sFv did not significantly increase either C8 or H2 sFv intrabody's stability as it might have been expected (Mhashilkar et al., 1995).

Taken together, the steady-state protein expression and the turnover rate analysis of the C8 and H2 sFv intrabodies indicate that the stability of an intrabody is a critical factor determining its efficiency in redirecting a target protein (Fig. 5). This is also evidenced by the lower level association of H2 sFv-nls intrabodies with caspase-7-FLAG in the coimmunoprecipitation assay (Fig. 4). It should be noted that the in vivo protein turnover rate determined in this study was also consistent with preliminary protein stability data measured by an in vitro heat denaturation experiment. Monitoring changes in their circular dichroism spectra as a function of temperature, it was observed that the thermal-unfolding transition temperature of purified, bacterially expressed C8 sFv is higher than that of H2 sFv (Boris A. Chrunyk, unpublished data).

3.5. Apoptotic signaling in stable sFv intrabody transfectants

In order to study the biological effects of retargeting caspase-7 to different cellular compartments, two anti-caspase-7 intrabody-expressing Jurkat cell lines were established, such that one expressed C8 sFv-nls intrabody and the other expressed C8 sFv-SKL intrabody. Expression of the intrabodies by these Jurkat cell lines was confirmed using immunofluorescence and pulse-chase experiments. Both C8 sFv-nls and C8 sFv-SKL intrabodies had over 8 h half-lives in the stable Jurkat cells (data not shown).

It has been reported that staurosporine can induce apoptosis and activate caspase-7 in Jurkat cells (Chinnaiyan et al., 1996). To test the possible effects of the anti-caspase-7 intrabodies on staurosporine-induced apoptosis in the Jurkat cell lines, the cell survival rate was determined after 18 h of treatment with 2 μM staurosporine. The percentage of cells that excluded Trypan Blue stain (indicating survival) was recorded in the presence or absence of staurosporine. Fig. 7 shows the average results from three experiments: cells expressing anti-caspase-7 C8

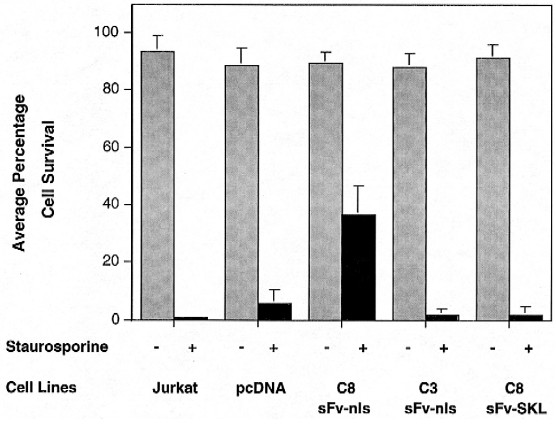

Fig. 7. Comparison of cell survival in different stable Jurkat cell lines following staurosporine treatment. Stable Jurkat cell lines were established by G418 selection of cells transfected with empty vector (pcDNA), C8 sFv-nls, C8 sFv-SKL, and a control intrabody C3 sFv-nls. These stable cell lines, along with the parental Jurkat cell line, were incubated in the same media with or without 2 μM staurosporine for 18 h at 37°C. The extent of cell survival was examined by Trypan Blue staining under a light microscope.

sFv-nls intrabodies had the highest survival rate among the cell lines tested while cells containing vector alone or cells possessing an irrelevant intrabody, C3 sFv-nls, exhibited little or no survival at 2 μM staurosporine. Note that the control C3 sFv-nls intrabody was as stable as the C8 sFv-nls intracellularly (data not shown). The incomplete sequestration of caspase-7 by the intrabodies (Figs. 3 and 5A) may have contributed to the less than complete resistance of the C8 sFv-nls expressing cell line to staurosporine, and may also underlie the susceptibility of the C8 sFv-SKL expressing cell line to the induction of apoptosis. These results demonstrate that sequestration of caspase-7 in the nucleus by a specific nucleus-directed intrabody can inhibit the biological function(s) of caspase-7 in apoptosis, and these experiments furthermore suggest a critical role for caspase-7 in signaling the induction of apoptosis. These experiments thus serve to exemplify how intrabodies may be used to evaluate the biological functions of target antigens in their natural intracellular milieu.

4. Discussion

Intrabodies have been used widely for both phenotypic and functional knockouts of target proteins. Unlike previously reported cases, where an intrabody was used to block the normal intracellular trafficking of a target protein (Marasco et al., 1993; Beerli et al., 1994; Deshane et al., 1994; Mhashilkar et al., 1995), the present investigation emphasizes that specific intrabodies can modulate the properties of a target cell by successfully redirecting the antigen to a particular subcellular compartment. Using transient transfection analysis, we studied two anti-caspase-7 sFv intrabodies and their effects on caspase-7. The anti-caspase-7 sFv intrabodies were fused to distinct trafficking signals for either nuclear, peroxisomal, or ER targeting and each of these sFv fusions was expressed in the intended subcellular compartment. When used to redirect the intracellular localization of cotransfected cytosolic caspase-7 protein, both intrabodies were able to target caspase-7 through direct protein-protein interactions to different cellular compartments, as governed by the subcellular targeting signal attached to the specific intrabody. The C8 sFv intrabodies were found to be significantly more stable than the H2 sFv intrabodies, which had a dramatic impact on their relative effectiveness. The intrabody with a longer half-life and higher steady-state protein level was far more effective in the sequestration of cotransfected caspase-7. The studies presented here do not provide significant insights into how the epitopes recognized by different sFv intrabodies may impact their effectiveness. However, it appears unlikely that the specific epitopes recognized in this study were critical to the effectiveness of the sFv, since the mechanism of sequestration was due to protein-protein interactions and the lower affinity intrabody was clearly the most effective. Finally, the expression of a nuclear-targeted anti-caspase-7 sFv intrabody, acting on the endogenous caspase-7 in a stable Jurkat cell line, resulted in an increased cell survival upon staurosporine treatment, suggesting functional blockage of apoptosis due to nuclear sequestration of caspase-7. No significant cell survival was observed in cells expressing the peroxisome-targeted anti-caspase-7 sFv intrabody. This is consistent with the observation that the sequestration of cytosolic caspase-7 within peroxisomes was incomplete, as evidenced by the substantial amount of cytosolic staining for caspase-7 (Fig. 3C). It is likely that the capacity of the peroxisomes or peroxisomal transport mechanism limited the complete sequestration of caspase-7 in this case. It also cannot be ruled out at present that successfully blocking the induction of apoptosis depends both upon the site of subcellular sequestration and the choice of apoptotic stimulus.

Recent evidence on caspases indicates that these cysteinyl aspartate-specific proteinases play key roles in mediating apoptosis (Cohen, 1997; Nicholson and Thornberry, 1997). All caspases appear to share a similar proenzyme organization, and upon stimulation by apoptotic signals, they are proteolytically released from their proenzyme forms. In the case of caspase-7, it is known that apoptotic stimuli induce its cleavage from the proenzyme p35 form to an active heterodimer comprising p20 and p12 (Chinnaiyan et al., 1996; Duan et al., 1996). Such cleavage events occur in the cytosol and result in the production of active caspases. The active forms of caspases then cleave key cellular structural components, resulting in the systematic disassembly of the

cell, termed apoptosis. In this study, anti-caspase-7 sFv intrabodies successfully redirected caspase-7 to nuclei and peroxisomes from the cytosol of the transfected cells (Fig. 3). The altered subcellular localization of caspase-7 in cells cotransfected with its sFv intrabodies was the result of direct protein-protein interactions between the target antigen and the specific intrabody (Fig. 4). Sequestration of the caspase-7 in the cell nucleus would be expected to render the caspase-7 inaccessible to the other proteins in its pathway. The most dramatic manifestation of such functional blockage was the significant increase in cell survival, in the presence of 2 μM staurosporine, by Jurkat cells stably expressing the nuclear-targeted anti-caspase-7 sFv intrabody (Fig. 7). It may be postulated that such blockage results from either the inability to activate the nuclear-localized caspase-7 proenzyme or the inability of the nuclear-localized caspase-7 to reach its substrate. This could lead to either a complete inhibition of apoptosis or a delay of apoptosis due to the altered kinetics.

In the past, the same primary criteria were assumed to apply when choosing an sFv in applications for extracellular targeting or as an intrabody, namely, the specificity and antigen-binding affinity of the sFv binding site. However, this investigation indicates that these criteria are insufficient to predict the effectiveness of intrabody retargeting its antigen (Fig. 5 and Table 1). As summarized in Table 1, the lower affinity anti-caspase-7 antibody, C8 sFv, had a much longer intracellular half-life than that of H2 sFv. This resulted in a significant accumulation of C8 sFv within transfected cells that yielded antigen retargeting which was far superior to that mediated by H2 sFv, even though the latter had a higher affinity against caspase-7 and a much faster association rate constant. It should be noted that results from additional studies of two other sFv intrabodies against a different cellular target are also consistent with this observation. In this alternative case, two distinct sFv had roughly comparable affinities in vitro, but one exhibited a half-life of over 8 h, while the other had a $t_{1/2}$ of less than 2 h inside mammalian cells. As in the case of C8 sFv, the stable sFv intrabody was far more effective in directing its target to different subcellular compartments than the sFv with a shorter half-life (manuscript in preparation). Although it is possible that affinity of an sFv intrabody inside of a cell might be different from the value measured in vitro by a BIAcore and could thus influence its efficiency on the target in vivo, our data consistently showed a strong correlation between targeting efficiency and the turnover rate as well as the related steady-state protein accumulation of an sFv intrabody. These results suggest that turnover rate, as an index of overall stability, and steady-state accumulation of an intrabody are highly critical determinants of its efficacy. This consideration should be taken together with affinity and specificity to provide a useful description of an intrabody. This conclusion should apply not only to an intrabody used to sequester the target antigen within an inaccessible site, but should also apply to an intrabody that inactivates enzyme activity or disrupts intracellular protein–protein interactions by competitive inhibition. In these latter cases, the steady-state concentration and antigen-binding affinity of an intrabody would govern the extent of its binding to critical contact surfaces on the target antigen, and thus disruption of normal target interactions, which would necessarily be determined by thermodynamic considerations. While it remains to be determined what structural properties of sFv intrabodies underlie their stability, the parameters described in this investigation offer valuable criteria for choosing an optimal sFv for use as an intrabody. Our findings suggest the future development of optimal intrabodies will benefit from the efforts that have been made recently to develop highly stable Fv frameworks (Jung and Plückthun, 1997; Nieba et al., 1997; Jager and Plückthun, 1999). Ultimately, special sFv-phage display libraries may be designed that consistently yield effective sFv intrabodies.

Acknowledgements

Alexandra Huhalov and Jin Yao contributed equally to this project. Wayne A. Marasco made contributions in his capacity as a consultant to IntraImmune Therapies, The authors wish to thank Daniel C. McKenna, for his excellent technical assistance in the construction of Jurkat cell lines that stably expressed the sFv intrabodies, and Boris A. Chrunyk, for sharing his unpublished data on sFv thermal denaturation.

References

Beerli, R.R., Wels, W., Hynes, N.E., 1994. Intracellular expression of single chain antibodies reverts ErbB-2 transformation. J. Biol. Chem. 269, 23931–23936.

Biocca, S., Pierandrei-Amaldi, P., Cattaneo, A., 1993. Intracellular expression of anti-p21 ras single chain Fv fragments inhibits meiotic maturation of xenopus oocytes. Biochem. Biophys. Res. Commun. 197, 422–427.

Biocca, S., Pierandrei-Amaldi, P., Campioni, N., Cattaneo, A., 1994. Intracellular immunization with cytosolic recombinant antibodies. Biotechnology (NY) 12, 396–399.

Bird, R.E., Hardman, K.D., Jacobson, J.W., Johnson, S., Kaufman, B.M., Lee, S.M., Lee, T., Pope, S.H., Riordan, G.S., Whitlow, M., 1988. Single-chain antigen-binding proteins. Science 242, 423–426.

Chinnaiyan, A.M., Orth, K., O'Rourke, K., Duan, H., Poirier, G.G., Dixit, V.M., 1996. Molecular ordering of the cell death pathway. Bcl-2 and Bcl-xL function upstream of the CED-3-like apoptotic proteases. J. Biol. Chem. 271, 4573–4576.

Cochet, O., Kenigsberg, M., Delumeau, I., Virone-Oddos, A., Multon, M.C., Fridman, W.H., Schweighoffer, F., Teillaud, J.L., Tocque, B., 1998. Intracellular expression of an antibody fragment-neutralizing p21 ras promotes tumor regression. Cancer Res. 58, 1170–1176.

Cohen, G.M., 1997. Caspases: the executioners of apoptosis. Biochem. J. 326, 1–16.

Deshane, J., Loechel, F., Conry, R.M., Siegal, G.P., King, C.R., Curiel, D.T., 1994. Intracellular single-chain antibody directed against erbB2 down-regulates cell surface erbB2 and exhibits a selective anti-proliferative effect in erbB2 overexpressing cancer cell lines. Gene Ther. 1, 332–337.

Deshane, J., Cabrera, G., Grim, J.E., Siegal, G.P., Pike, J., Alvarez, R.D., Curiel, D.T., 1995a. Targeted eradication of ovarian cancer mediated by intracellular expression of anti-erbB-2 single-chain antibody. Gynecol. Oncol. 59, 8–14.

Deshane, J., Siegal, G.P., Alvarez, R.D., Wang, M.H., Feng, M., Cabrera, G., Liu, T., Kay, M., Curiel, D.T., 1995b. Targeted tumor killing via an intracellular antibody against erbB-2. J. Clin. Invest. 96, 2980–2989.

Deshane, J., Grim, J., Loechel, S., Siegal, G.P., Alvarez, R.D., Curiel, D.T., 1996. Intracellular antibody against erbB-2 mediates targeted tumor cell eradication by apoptosis. Cancer Gene Ther. 3, 89–98.

Deshane, J., Siegal, G.P., Wang, M., Wright, M., Bucy, R.P., Alvarez, R.D., Curiel, D.T., 1997. Transductional efficacy and safety of an intraperitoneally delivered adenovirus encoding an anti-erbB-2 intracellular single-chain antibody for ovarian cancer gene therapy. Gynecol. Oncol. 64, 378–385.

Duan, H., Chinnaiyan, A.M., Hudson, P.L., Wing, J.P., He, W.-W., Dixit, V.M., 1996. ICE-LAP3, a novel mammalian homologue of the *Caenorhabditis elegans* cell death protein Ced-3 is activated during Fas- and tumor necrosis factor-induced apoptosis. J. Biol. Chem. 271, 1621–1625.

Gould, S.J., Keller, G.A., Hosken, N., Wilkinson, J., Subramani, S., 1989. A conserved tripeptide sorts proteins to peroxisomes. J. Cell Biol. 108, 1657–1664.

Graus-Porta, D., Beerli, R.R., Hynes, N.E., 1995. Single-chain antibody-mediated intracellular retention of ErbB-2 impairs Neu differentiation factor and epidermal growth factor signaling. Mol. Cell Biol. 15, 1182–1191.

Greenman, J., Jones, E., Wright, M.D., Barclay, A.N., 1996. The use of intracellular single-chain antibody fragments to inhibit specifically the expression of cell surface molecules. J. Immunol. Methods 194, 169–180.

Haber, E., 1992. Engineered antibodies as pharmacological tools. Immunol. Rev. 130, 189–212.

Hammond, C., Helenius, A., 1995. Quality control in the secretory pathway. Curr. Opin. Cell Biol. 7, 523–529.

Hopp, T.P., Prickett, K.S., Price, C., Libby, R.T., March, C.J., Cerretti, P., Urdal, D.L., Conlon, P.J., 1988. A short marker sequence useful for recombinant protein identification and purification. Biotechnology 6, 1205–1210.

Huston, J.S., Levinson, D., Mudgett-Hunter, M., Tai, M.S., Novotny, J., Margolies, M.N., Ridge, R.J., Bruccoleri, R.E., Haber, E., Crea, R., Oppermann, H., 1988. Protein engineering of antibody binding sites: recovery of specific activity in an anti-digoxin single-chain Fv analogue produced in Escherichia coli. Proc. Natl Acad. Sci. U.S.A. 85, 5879–5883.

Huston, J.S., Margolies, M.N., Haber, E., 1996. Antibody binding sites. Adv. Protein Chem. 49, 329–450.

Jager, M., Plückthun, A., 1999. Folding and assembly of an antibody Fv fragment, a heterodimer stabilized by antigen. J. Mol. Biol. 285, 2005–2019.

Jannot, C.B., Beerli, R.R., Mason, S., Gullick, W.J., Hynes, N.E., 1996. Intracellular expression of a single-chain antibody directed to the EGFR leads to growth inhibition of tumor cells. Oncogene 13, 275–282.

Jones, S.D., Marasco, W.A., 1998. Antibodies for targeted gene therapy: extracellular gene targeting and intracellular expression. Adv. Drug Delivery Rev. 31, 153–170.

Jung, S., Plückthun, A., 1997. Improving in vivo folding and stability of a single-chain Fv antibody fragment by loop grafting. Protein Eng. 10, 959–966.

Kalderon, D., Roberts, B.L., Richardson, W.D., Smith, A.E., 1984. A short amino acid sequence able to specify nuclear location. Cell 39, 499–509.

Keller, G.-A., Krisans, S., Gould, S.J., Sommer, J.M., Wang, C.C., Schilebs, W., Kunau, W., Brody, S., Subramani, S., 1991. Evolutionary conservation of a microbody targeting signal that targets proteins to peroxisomes, glyoxysomes, and glycosomes. J. Cell Biol. 114, 893–904.

Marasco, W.A., 1997. Intrabodies: turning the humoral immune system outside in for intracellular immunization. Gene Ther. 4, 11–15.

Marasco, W.A., Haseltine, W.A., Chen, S.Y., 1993. Design, intracellular expression, and activity of a human anti-human immunodeficiency virus type 1 gp120 single-chain antibody. Proc. Natl. Acad. Sci. U.S.A. 90, 7889–7893.

Marks, C., Marks, J.D., 1996. Phage libraries — a new route to clinically useful antibodies. N. Engl. J. Med. 335, 730–733.

Marks, J.D., Hoogenboom, H.R., Bonnert, T.P., McCafferty, J., Griffiths, A.D., Winter, G., 1991. By-passing immunization. Human antibodies from V-gene libraries displayed on phage. J. Mol. Biol. 222, 581–597.

Mhashilkar, A.M., Bagley, J., Chen, S.Y., Szilvay, A.M., Helland,

D.G., Marasco, W.A., 1995. Inhibition of HIV-1 Tat-mediated LTR transactivation and HIV-1 infection by anti-Tat single chain intrabodies. EMBO J. 14, 1542–1551.

Mhashilkar, A.M., Biswas, D.K., LaVecchio, J., Pardee, A.B., Marasco, W.A., 1997. Inhibition of human immunodeficiency virus type 1 replication in vitro by a novel combination of anti-tat single-chain intrabodies and NF-κB antagonists. J. Virol. 71, 6486–6494.

Montano, X., Jimenez, A., 1995. Intracellular expression of the monoclonal anti-ras antibody Y13-259 blocks the transforming activity of ras oncogenes. Cell Growth Differ. 6, 597–605.

Munro, S., Pelham, H.R.B., 1987. A C-terminal signal prevents secretion of luminal ER proteins. Cell 48, 899–907.

Nicholson, D.W., Thornberry, N.A., 1997. Caspases: killer proteases. Trends Biochem. Sci. 22, 299–306.

Nieba, L., Honegger, A., Krebber, C., Plückthun, A., 1997. Disrupting the hydrophobic patches at the antibody variable/constant domain interface: improved in vivo folding and physical characterization of an engineered scFv fragment. Protein Eng. 10, 435–444.

Pelegrin, M., Marin, M., Noel, D., Piechaczyk, M., 1998. Genetically engineered antibodies in gene transfer and gene therapy. Hum. Gene Ther. 9, 2165–2175.

Pelham, H.R.B., 1989. Control of protein exit from the endoplasmic reticulum. Annu. Rev. Cell Biol. 5, 1–23.

Richardson, J.H., Sodroski, J.G., Waldmann, T.A., Marasco, W.A., 1995. Phenotypic knockout of the high-affinity human interleukin 2 receptor by intracellular single-chain antibodies against the alpha subunit of the receptor. Proc. Natl. Acad. Sci. U.S.A. 92, 3137–3141.

Richardson, J.H., Waldmann, T.A., Sodroski, J.G., Marasco, W.A., 1997. Inducible knockout of the interleukin-2 receptor alpha chain: expression of the high-affinity IL-2 receptor is not required for the in vitro growth of HTLV-I-transformed cell lines. Virology 237, 209–216.

Rondon, I.J., Marasco, W.A., 1997. Intracellular antibodies (intrabodies) for gene therapy of infectious diseases. Annu. Rev. Microbiol. 51, 257–283.

Vaughan, T.J., Williams, A.J., Pritchard, K., Osbourn, J.K., Pope, A.R., Earnshaw, J.C., McCafferty, J., Hodits, R.A., Wilton, J., Johnson, K.S., 1996. Human antibodies with sub-nanomolar affinities isolated from a large non-immunized phage display library. Nat. Biotechnol. 14, 309–314.

Werge, T.M., Baldari, C.T., Telford, J.L., 1994. Intracellular single chain Fv antibody inhibits Ras activity in T-cell antigen receptor stimulated Jurkat cells. FEBS Lett. 351, 393–396.

Wiemer, E.A.C., Wenzel, T., Deerinck, T.J., Ellisman, M.H., Subramani, S., 1997. Visualization of the peroxisomal compartment in living mammalian cells: dynamic behavior and association with microtubules. J. Cell Biol. 136, 71–80.

Winter, G., Griffiths, A.D., Hawkins, R.E., Hoogenboom, H.R., 1994. Making antibodies by phage display technology. Annu. Rev. Immunol. 12, 433–455.

Yuan, Q., Strauch, K.L., Lobb, R.R., Hemler, M.E., 1996. Intracellular single-chain antibody inhibits integrin VLA-4 maturation and function. Biochem. J. 318, 591–596.